Bioorganic & Medicinal Chemistry xxx (2018) xxx–xxx

Contents lists available at ScienceDirect

Bioorganic & Medicinal Chemistry

journal homepage: www.elsevier.com/locate/bmc

PET probe detecting non-small cell lung cancer susceptible to epidermal growth factor receptor tyrosine kinase inhibitor therapy

Akira Makino [a,b,*], Anna Miyazaki [a], Ayaka Tomoike [a], Hiroyuki Kimura [a,c], Kenji Arimitsu [c], Masahiko Hirata [d], Yoshiro Ohmomo [d], Ryuichi Nishii [e], Hidehiko Okazawa [b], Yasushi Kiyono [b], Masahiro Ono [a], Hideo Saji [a,*]

[a] Graduate School of Pharmaceutical Sciences, Kyoto University, 46-29 Yoshida-Adachi-cho, Sakyo-ku, Kyoto 6068501, Japan
[b] Biomedical Imaging Research Center (BIRC), University of Fukui, 23-3 Matsuoka-shimoaizuki, Eiheiji-cho, Yoshida-gun, Fukui 9101193, Japan
[c] Department of Analytical and Bioinorganic Chemistry, Kyoto Pharmaceutical University, Kyoto 6078414, Japan
[d] Graduate School of Pharmaceutical Sciences, Osaka University of Pharmaceutical Sciences, Osaka 5691041, Japan
[e] National Institute of Radiological Sciences, Chiba 2638555, Japan

ARTICLE INFO

Article history:
Received 2 November 2017
Revised 6 February 2018
Accepted 7 February 2018
Available online xxxx

Keywords:
Epidermal growth factor receptor
EGFR L858R and T790M mutations
Tyrosine kinase inhibitor
Positron emission tomography
In vivo imaging

ABSTRACT

Tyrosine kinase inhibitors for epidermal growth factor receptor (EGFR-TKIs) are used as molecular targeted therapy for non-small cell lung cancer (NSCLC) patients. The therapy is applied to the patients having EGFR-primary L858R mutation, but drug tolerance caused by EGFR-secondary mutation is occurred within one and half years. For the non-invasive detection of the EGFR-TKIs treatment positive patients by positron emission tomograpy (PET) imagaing, fluorine-18 labeled thienopyrimidine derivative, **[^{18}F]FTP2** was newly synthesized. EGFR inhibition assay, cell uptake study, and blocking study indicated **[^{18}F]FTP2** binds with high and selective affinity for EGFR with L858R mutation, and not with L858R/T790M dual mutations. On animal PET study using tumor bearing mice, H3255 cells expressing L858R mutated EGFR was more clearly visualized than H1975 cells expressing L858R/T790M dual mutated EGFR. **[^{18}F]FTP2** has potential for detecting NSCLC which is susceptible to EGFR-TKI treatment.

1. Introduction

World Health Organization (WHO) reported lung cancer is the leading cause of cancer death worldwide, accounting for 1.69 million deaths in 2015. It can be categorized to small cell lung cancer (SCLC) and non-small cell lung cancer (NSCLC), and the treatment is varied depending on the cancer type and stage. In case of stage IIIB or IV NSCLC, the epidermal growth factor receptor-tyrosine kinase inhibitor (EGFR-TKI) such as gefitinib and erlotinib is one treatment option. EGFR-TKIs can block signal transmission for cancer cells proliferation and suppress the growth.[1] Especially, they work effectively to the patient whose EGFR-tyrosine kinase have primary mutation such as L858R in exon 21 and exon 19 deletion.[2–4] Therefore, detection of the EGFR mutation by biopsy test is essential for the treatment policy determination. However, the problem is EGFR-TKI treatment induces drug tolerance within about one and a half years after the start of the treatment, and 60% of the cause is a secondary mutation of EGFR-T790M.[5–7] On clinical site, genetic examination by biopsy will be conducted after cancer exacerbation is occurred during the treatment, and presence or absence of the EGFR secondary mutation is investigated. This is because biopsy test is invasive and cannot be performed so frequently. When the T790M mutation becomes positive, the treatment is switched to platinum preparations and/or osimertinib,[8–10] which is EGFR T790M mutation-positive metastatic NSCLC therapeutic drug. Recently, liquid biopsy is also utilized for the detection of T790M mutation, but there is a time lag between occurrence of the second mutation caused drug tolerance and switching of the treatment policy.

As PET tracers detecting EGFR overexpressing on NSCLC, radiolabeled gefitinib and erlotinib derivatives are developed.[11–13] However, it has also been reported that these probes are not suitable for detecting drug tolerance of EGFR-TKIs.[14] Development of a new PET probe which can detect EGFR-TKIs treatment response NSCLC is important because periodic PET examination for patients undergoing EGFR-TKI treatment enables early detection of the drug tolerance, and helps prompt modification of the treatment strategy. In our group, radiofluorinated 4-(anilino)pyrido[3,4-*d*]pyrimidine derivative, [^{18}F]APP-1 was synthesized which shows potential to

* Corresponding authors at: Biomedical Imaging Research Center (BIRC), University of Fukui, 23-3 Matsuoka-shimoaizuki, Eiheiji-cho, Yoshida-gun, Fukui 9101193, Japan (A. Makino).
E-mail addresses: amakino@u-fukui.ac.jp (A. Makino), hsaji@pharm.kyoto-u.ac.jp (H. Saji).

https://doi.org/10.1016/j.bmc.2018.02.007
0968-0896/

be used as a PET tracer to discriminate between L858R and L858R/T790M mutant EGFRs in NSCLC.[15] However, APP-1 has weak inhibition ability against L858R/T790M mutated EGFR (IC_{50} = 326 ± 64 nM). Therefore, development of a new PET tracer with higher selectivity against L858R and L858R/T790M mutated EGFRs is performed in this study.

2. Results and discussion

2.1. Probe design

Thienopyrimidine derivatives, which are reported to be inhibitors against wild type and primary mutated EGFRs, but not against secondary mutated EGFR, was selected as the mother nucleus structure on this study.[16–19] Fluorine-18 was chosen as positron nuclides, which has a relatively long half-life time of 110 min. Candidate compounds designed (**FTPs1–5**) were listed in Fig. 1. **FTP1** has a simple structure to introduce fluorine-18 on the piperidine ring via ethyl linker. EGFR tyrosine kinase inhibitors of HKI-272, EKB-569 and BIBW2992 have a Michael acceptor group, which plays a crucial role in inhibiting EGFR via irreversibly covalent bond formation with cysteine residue.[20–23] To the **FTP2**, Michael addition unit was inserted. In order to evaluate the effectiveness of Michael acceptor unit, **FTP3** and **FTP4** were designed in which labeling sites are linked with two different alkyl chains. **FTP5** was converted methylol unit in **FTP2** to methyl group for simplification of the synthetic route.

Chemical synthetic procedures of these five non-radiolabeled candidate compounds are summarized in Supporting information.

2.2. Evaluation of inhibitory potency of *FTPs1-5* in vitro

The inhibition ability of **FTPs1-5** and gefitinib on EGFR tyrosine kinase activity was evaluated using Promega ADP-Glo Kinase Assay kit.[24] IC_{50} values against wild type and three types of mutated EGFR were summarized in Table 1. **FTP2** and **FTP5** showed low IC_{50} values against wild type and L858R mutated EGFRs. IC_{50} value of **FTP2** against L858R mutated EGFRs was 9 nM, whose value is lower than that of gefitinib. The influence of the methylol unit substitution to methyl group is limited, but IC_{50} value of **FTP5** against L858R mutated EGFRs was increased to 27 nM. The high IC_{50} value of **FTPs3** and **4** indicate Michael acceptor group in **FTPs2** and **5** works effectively for the kinase activity inhibition. Importantly, almost all compounds didn't show inhibitory activity against EGFRs including T790M gefitinib negative mutation. IC_{50} value of **FTP2** against T790M EGFR was 8966 nM, which is ca. 1000 times higher than that against L858R EGFR. Because of the excellent IC_{50} value of **FTP2** against L858R mutated EGFR, **FTP2** was selected for the further evaluations.

2.3. Radiosynthesis

[^{18}F]FTP2 was synthesized by two steps reaction using [^{18}F]2-fluoroethyl tosylate, which was prepared from 1,2-ditosylethane in acetonitrile solution in the presence of Kryptofix222 and potassium carbonate (Fig. 2a). The overall radiochemical yield and radiochemical purity of **[^{18}F]FTP2** was 6.8%, and >99%, respectively. Molar specific activity of **[^{18}F]FTP2** was 50 GBq/μmol at minimum.

[^{18}F]FTP2 was incubated in sarin and blood serum for 1 h, but no metabolized compounds were detected from HPLC analysis, indicating **[^{18}F]FTP2** is stable *in vitro* condition (Fig. 2b).

2.4. Cell uptake study

NCI-H3255 and NCI-H1975 are human NSCLC cell lines expressing L858R mutated and L858R/T790M dual mutated EGFR, respectively. To the cultures of these two NSCLC cells, **[^{18}F]FTP2** was incubated, and amount of **[^{18}F]FTP2** uptake into the cell was evaluated (Fig. 3a). Amount of up taken **[^{18}F]FTP2** into H3255

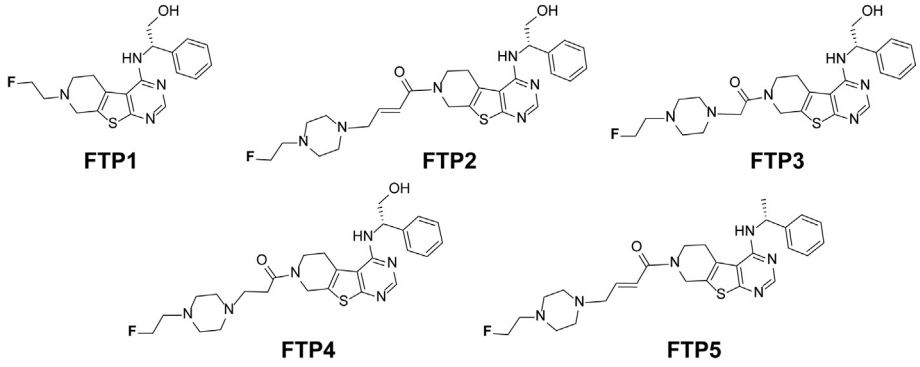

Fig. 1. Probe candidate compounds **FTPs1–5** for L858R mutated epidermal growth factor receptor (EGFR) detection.

Table 1
Epidermal growth factor receptor-tyrosine kinase (EGFR-TK) inhibition assay using Promega ADP-Glo Kinase Assay kit (n = 3).

Compound	EGFR kinase inhibition: IC_{50} value (nM). Numbers in parentheses are logIC_{50} (nM) ± standard error (n = 3)			
	WT	L858R	T790M	DM (L858R/T790M)
FTP1	2309 (3.363 ± 0.316)	3414 (3.533 ± 0.076)	Inactive	Inactive
FTP2	44 (1.643 ± 0.094)	9 (0.953 ± 0.039)	8966 (3.953 ± 0.122)	Inactive
FTP3	4370 (3.640 ± 0.278)	2674 (3.427 ± 0.266)	Inactive	Inactive
FTP4	2827 (3.451 ± 0.105)	1835 (3.264 ± 0.379)	Inactive	Inactive
FTP5	130 (2.114 ± 0.186)	27 (1.434 ± 0.090)	Inactive	Inactive
Gefitinib	20 (1.301 ± 0.056)	21 (1.314 ± 0.037)	868 (2.938 ± 0.047)	7111 (3.852 ± 0.103)

IC_{50} values greater than 10 μM are indicated as "inactive".

Please cite this article in press as: Makino A., et al. Bioorg. Med. Chem. (2018), https://doi.org/10.1016/j.bmc.2018.02.007

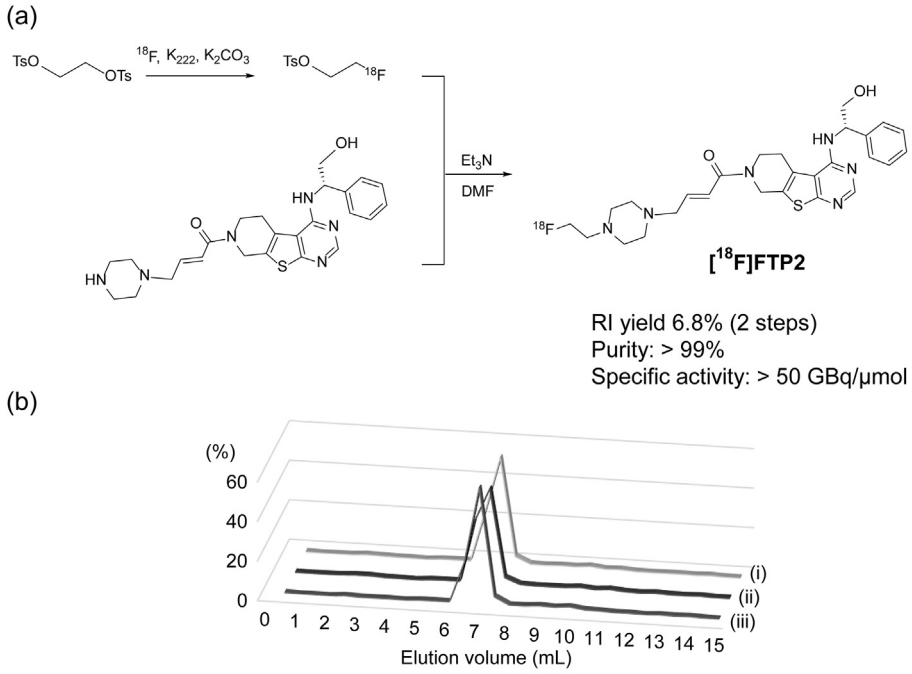

Fig. 2. (a) Radiosynthesis of **[^{18}F]FTP2** and (b) HPLC chromatogram of (i) **[^{18}F]FTP2**, (ii) **[^{18}F]FTP2** incubated in blood serum for 1 h, and (iii) **[^{18}F]FTP2** incubated in saline for 1 h. Y-axis indicates the relative amount of radioactivity contained in each fractions (0.50 mL/fractions).

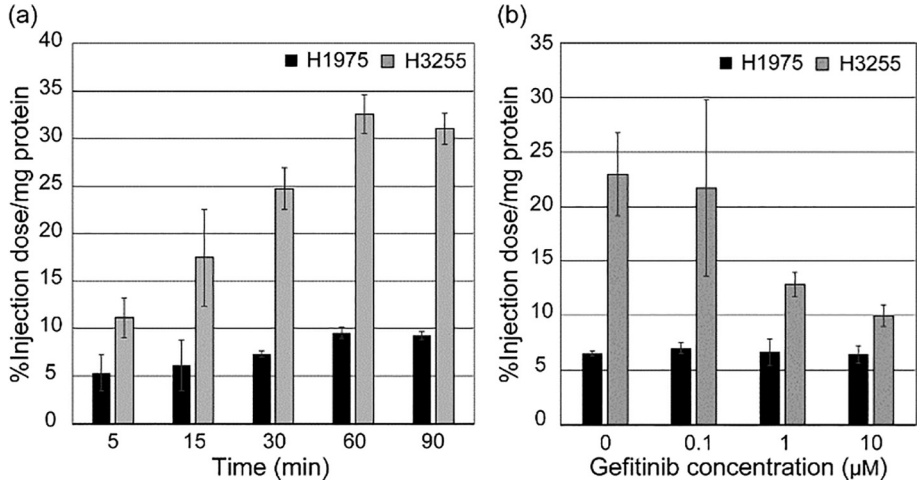

Fig. 3. (a) Time courses of **[^{18}F]FTP2** uptake by H1975 and H3255 cells and (b) uptake of **[^{18}F]FTP2** after 30 min incubation with or without gefitinib (0.1–10 μM).

was reached to over 32.5 ± 2.0%ID/mg protein after 60 min from the incubation, which is three times higher than that into H1975 (9.51 ± 0.6%ID/mg protein). Furthermore, the H3255 cell uptake was decreased below half from the original by addition of 0.1–10 μM gefitinib as inhibitor, whereas the H1975 was not changed, indicating **[^{18}F]FTP2** uptake into H3255 is considered to be specific binding to L858R mutated EGFR (Fig. 3b). Residual **[^{18}F]FTP2** into H1975 and H3255 cells, which does not reduce by addition of excess amount of inhibitors, show nonspecific binding.

2.5. In vivo imaging

[^{18}F]FTP2 was intravenously administrated to the BALB/c nude mice subcutaneously transplanted with H3255 and H1975 cells, and positron images were acquired during 180–200 min from the dosage using animal PET/CT system (Fig. 4). Accumulation of **[^{18}F]FTP2** to H3255 cell transplanted region was observed, but not to H1975. Biodistribution of **[^{18}F]FTP2** at 180 min from the dosage is shown in Table 2. The accumulation of **[^{18}F]FTP2** in H3255 tumor region was 2.5 ± 0.3%ID/g, which is 2.7 times higher than that in H1975 tumor region (0.9 ± 0.1%ID/g). In organs other than the transplanted tumor cells, similar ^{18}F distribution was observed. The high accumulation in the intestine is considered to be caused by relatively hydrophobic structure of **FTP2**. **[^{18}F]FTP2** is trapped in the reticuloendothelial system such as liver, and then transferred to the intestine via bile excretion. In case of H3255 bearing mice, tumor to blood, muscle and lung signal intensity ratio was reached to 3.21, 5.50, and 2.53, respectively. On the other hand, those value of H1975 bearing mice was 1.25, 2.00 and 0.90, respectively.

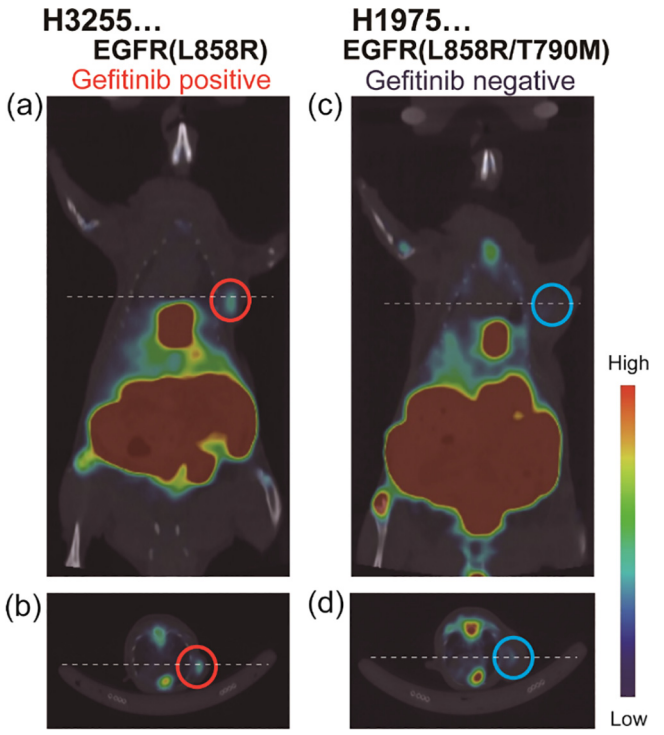

Fig. 4. PET-CT image of **[^{18}F]FTP2** in (a, b) H3255 (EGFR L858R, gefitinib positive) and (c, d) H1975 (EGFR L858R/T790M gefitinib negative) bearing mice at 3 h post-injection. Panels (a, c) and (b, d) show coronal and transverse images, respectively.

Table 2
Biodistribution of **[^{18}F]FTP2** in tumor bearing mice after 3 h from the dosage. The values represent the mean ± SD (n = 5).

Tissue (% ID/g)	H3255 EGFR (L858R)	H1975 EGFR (L858R/T790M)
Blood	0.76 ± 0.07	0.74 ± 0.08
Spleen	0.70 ± 0.09	0.80 ± 0.13
Pancreas	0.56 ± 0.10	0.63 ± 0.06
Stomach	1.19 ± 0.33	1.30 ± 0.32
Intestine	38.8 ± 8.0	41.0 ± 6.0
Kidney	0.93 ± 0.10	0.94 ± 0.09
Liver	1.44 ± 0.12	1.39 ± 0.12
Lung	0.98 ± 0.10	1.02 ± 0.17
Heart	0.56 ± 0.13	0.61 ± 0.10
Tumor	2.47 ± 0.34	0.92 ± 0.08
Muscle	0.45 ± 0.05	0.46 ± 0.04
Bone	2.44 ± 0.51	2.11 ± 0.80
Accumulation ratio		
Tumor/Blood	3.21	1.25
Tumor/Muscle	5.50	2.00
Tumor/Lung	2.53	0.90

2.6. In vivo blocking study

[^{18}F]FTP2 was co-injected with excess amount of gefitinib (500 μM) to the H3255 or H1975 bearing mice, and radioactivity accumulated at these tumor regions was evaluated by organ harvesting method after three hours from the dosage. As shown in Fig. 5, the **[^{18}F]FTP2** accumulation in H3255 cells was significantly reduced to the 37% from the control, but that in H1975 was not changed. These results were well-correlated with *in vitro* cell uptake study shown in Fig. 3, indicating **[^{18}F]FTP2** selectively binds to L858R mutated EGFR.

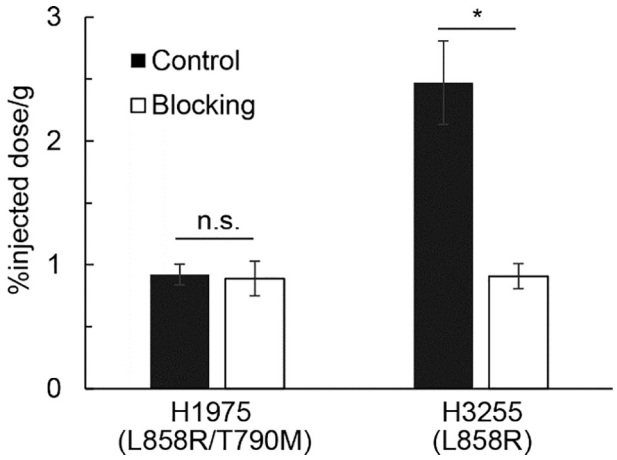

Fig. 5. Effect of co-injection of gefitinib on biodistribution of **[^{18}F]FTP2** (3h post-injection). The graphs show the mean %ID/g with error bars giving the standard deviation ($^{*}P < 0.01$).

3. Conclusion

Thienopyrimidine derivatives of **FTPs1-5** were newly designed and synthesized as new PET probe candidate compounds for detecting gefitinib treatment sensitive NSCLC. **FTP2** having Michael acceptor unit in the structure showed high affinity (low IC_{50} value) to gefitinib sensitive EGFR tyrosine kinase with L858R mutation but high value to gefitinib resistant T790M mutation. The cell-uptake and *in vivo* blocking study show that **[^{18}F]FTP2** binds specifically to EGFR tyrosine kinase with gefitinib sensitive L858R mutation but not to the gefitinib resistant L858R/T790M mutation. *In vivo* study indicates **[^{18}F]FTP2** can clearly visualize H3255 NSCLC expressing L858R mutated EGFR tyrosine kinase. **[^{18}F]FTP2** PET study is useful to the patients undergoing molecular target therapy with gefitinib. Accumulation of **[^{18}F]FTP2** indicates the NSCLC is sensitive against gefitinib treatment, and the reduction helps early detection of the occurrence of the EGFR secondary mutation, which causes drug tolerance. Therefore, **[^{18}F]FTP2** is a potential candidate compound for detecting gefitinib treatment sensitive NSCLC.

4. Experimental section

4.1. Instruments

Radiosynthesis was partly performed on JFE Hybrid synthesizer, cassette-type multipurpose automatic synthesizer module (JFE Engineering Corp., Tokyo, Japan). HPLC used was Prominence HPLC system (Shimadzu Corp., Kyoto, Japan). Radioactivity was measured by using 1480 Wizard 3 auto gamma counter (PerkinElmer, Waltham, MA, USA). PET scans were acquired by using a Triumph (TriFoil Imaging Inc., Chatsworth, CA, USA).

4.2. Enzyme assay

The inhibition ability of **FTPs1-5** on EGFR tyrosine kinase activity was performed using an ADP-Glo Lipid Kinase Assay kit (Promega, USA). The assay was carried out according to the ADP-Glo technical manual using purified recombinant EGFRs.

4.3. Radiosynthesis

For the syntheses, commercially available reagents and solvents were used without further purification. 2-[^{18}F]Fluoroethyltosylate

was synthesized using Hybrid synthesizer (JFE Engineering). Briefly, [^{18}F] fluoride solution containing 10 mg Kryptofix 2.2.2 (Sigma-Aldrich, St. Louis, USA) and 2.5 mg sodium carbonate (Sigma-Aldrich) was heated at 120 °C and the solvent was completely removed by repeated addition of acetonitrile. To the reaction vial, 1,2-bis(tosyloxy)ethane (20 mg) dissolved in acetonitrile (0.80 mL) was added, and the mixture was heated at 100 °C for 8 min. After the solution was diluted by 0.80 mL water, 2-[^{18}F]fluoroethyltosylate was isolated by COSMOSIL 5C$_{18}$-AR-II column (10 mm I.D. × 250 mm, Nacalai Tesque, Kyoto, Japan) by 50% acetonitrile aqueous solution as eluent (flow rate: 4.0 mL/min). Collected solution was diluted with water (15 mL), loaded on Sep-Pak C18 column, and dried with nitrogen gas flow. Radioactivity eluted from the Sep-Pak by acetonitrile (1.0 mL) was 6.4 × 10^2 MBq, and the total synthetic time was 69 min. Precursor (1.0 mg) dissolved in acetonitrile (0.11 mL), DMF (0.04 mL) and triethylamine (0.01 mL) was added. The reaction mixture was heated at 110 °C for 25 min, and then purified by HPLC using COSMOSIL 5C$_{18}$-AR-II column (10 mm I.D. × 250 mm). Acetonitrile/water containing 0.1% trifluoroacetic acid (v/v = 0 min: 15/85 → 5 min: 30/70 → 15 min: 35/65, flow rate: 5 mL/min) was used as eluent. The product was evaporated to dryness and dissolved in PBS (−) containing 1% DMSO to give **[^{18}F]FTP-2** (30 MBq). The total synthetic time (2 steps) was 158 min, and decay corrected yield was 6.8%. The radiochemical purity and specific activity of **[^{18}F]FTP-2** was over 99% and 51.8 GBq/μmol, respectively.

[^{18}F]FTP-2 solution (1 μL) was mixed saline or blood serum (100 μL), and incubated for 1 h. The mixture was centrifugated after addition of methanol (200 μL). The recovery rate from the blood serum was over 90%. The supernatant was analyzed by COSMOSIL 5C$_{18}$-AR-II column (4.6 mm I.D. × 150 mm) using acetonitrile/water containing 0.1% trifluoroacetic acid (v/v = 0 min: 20/80, 10 min: 30/70, flow rate: 1.0 mL/min) as eluent. The eluent was fractionated every 0.5 mL, and radioactivity included in each fractions against total one was measured.

4.4. Cell culture

H3255[25] and H1975, human derived lung adenocarcinoma, were provided by Dr. Juri G.Gelovani's lab., Dept. of Experimental Diagnostic Imaging, MD Anderson Cancer Center, Houston TX, in 2007, were cultured in Dulbecco's Modified Eagle Medium: Nutrient Mixture F-12 (DMEM/F12) (ThermoFisher Scientific, Waltham, MA, USA) supplemented with fetal bovine serum (FBS, 10% for H1975 and 20% for H3255) (ThermoFisher Scientific, Waltham, MA, USA) and 100 U/mL penicillin and 100 g/mL streptomycin under 37 °C in a well-humidified incubator with 5% CO_2 and 95% ambient air.

4.5. Cell uptake study

H1975 and H3255 NSCLC cells were cultured to confluence in 24 well plates. Cells were incubated in FBS-free DMEM/F12 medium containing **[^{18}F]FTP-2** (0.60 MBq/mL) with or without gefitinib (0.1–10 μM) for 30 min, and then washed three times with PBS (−) containing 1.0% DMSO. The cells were dissolved by 0.2 M sodium hydroxide solution, and the radioactivity was measured by automatic gamma counter. The protein concentration was measured using Pierce BCA Protein Assay kit (ThermoFisher Scientific, Waltham, MA, USA) and used for normalization.

4.6. Tumor model

Animal studies were conducted in accordance with our institutional guidelines, and the experimental procedures were approved by the Kyoto University and University of Fukui Animal Care Committees. Five-week-old male BALB/c nude mice were purchased from Japan SLC, Inc. (Hamamatsu, Japan). Tumor-model mice were prepared by subcutaneous injection of cells (1.0 × 10^7 H3255 cells or 3.0 × 10^6 H1975 cells in the right shoulder) suspended in 100 μL Matrigel™ (BD Biosciences, Franklin Lakes, NJ, USA). Approximately 4 weeks after implantation, the mice underwent tracer studies.

4.7. In vivo imaging and biodistribution study

On imaging, **[^{18}F]FTP-2** (9.1–14 MBq) in saline/0.5% Tween 80 was injected intravenously and PET scanning was started 3 h post-injection. Dynamic PET images were acquired for 20 min. The images were reconstructed using three-dimensional ordered subset expectation maximization (3D-OSEM). Soon after the PET imaging, the mouse were sacrificed and radioactivity in weighed tumors, blood, muscle, and lungs were measured using a γ counter.

On biodistribution study, **[^{18}F]FTP-2** (0.185 MBq) was injected intravenously into the tails of the tumor-bearing nude mice. For the blocking study, the gefitinib solution adjusted final concentration to be 500 μM was co-injected with **[^{18}F]FTP-2**. The mice were sacrificed at 3 h post-injection. Tumors and organs of interest were removed and weighed, and the radioactivity was measured.

Acknowledgments

This work was supported by the Practical Research for Innovative Cancer Control from the Japan Agency for Medical Research and Development (AMED) and Grants-in-Aid for Scientific Research from the Japan Society for the Promotion of Science.

A. Supplementary data

Supplementary data associated with this article can be found, in the online version, at https://doi.org/10.1016/j.bmc.2018.02.007.

References

1. Ono M, Hirata A, Kometani T, et al. *Mol Cancer Ther*. 2004;3:465–472.
2. Janku F, Garrido-Laguna I, Petruzelka LB, Stewart DJ, Kurzrock R. *J Thorac Oncol*. 2011;6:1601–1612.
3. Paez JG, Janne PA, Lee JC, et al. *Science*. 2004;304:1497–1500.
4. Rosell R, Carcereny E, Gervais R, et al. *Lancet Oncol*. 2012;13:239–246.
5. Kobayashi S, Boggon TJ, Dayaram T, et al. *N Engl J Med*. 2005;352:786–792.
6. Pao W, Miller VA, Politi KA, et al. *PLoS Med*. 2005;2:225–235.
7. Suda K, Mizuuchi H, Maehara Y, Mitsudomi T. *Cancer Metastasis Rev*. 2012;31:807–814.
8. Goss G, Tsai CM, Shepherd FA, et al. *Lancet Oncol*. 2016;17:1643–1652.
9. Mok TS, Wu YL, Ahn MJ, et al. *N Engl J Med*. 2017;376:629–640.
10. Liao BC, Lin CC, Lee JH, Yang JCH. *Lung Cancer*. 2017;110:7–13.
11. Bahce I, Smit EF, Lubberink M, et al. *Clin Cancer Res*. 2013;19:183–193.
12. Memon AA, Jakobsen S, Dagnaes-Hansen F, Sorensen BS, Keiding S, Nexo E. *Cancer Res*. 2009;69:873–878.
13. Seimbille Y, Phelps ME, Czernin J, Silverman DHS. *J Labelled Compd Radiopharm*. 2005;48:829–843.
14. Traxl A, Beikbaghban T, Wanek T, et al. *Nucl Med Biol*. 2017;52:7–15.
15. Kimura H, Okuda H, Ishiguro M, et al. *ACS Med Chem Lett*. 2017;8:418–422.
16. Bugge S, Buene AF, Jurisch-Yaksi N, et al. *Eur J Med Chem*. 2016;107:255–274.
17. Bugge S, Kaspersen SJ, Larsen S, et al. *Eur J Med Chem*. 2014;75:354–374.
18. Pedeboscq S, Gravier D, Casadebaig F, et al. *Eur J Med Chem*. 2010;45:2473–2479.
19. Waterson AG, Petrov KG, Hornberger KR, et al. *Bioorg Med Chem Lett*. 2009;19:1332–1336.
20. Kwak EL, Sordella R, Bell DW, et al. *Proc Natl Acad Sci USA*. 2005;102:7665–7670.
21. Li D, Ambrogio L, Shimamura T, et al. *Oncogene*. 2008;27:4702–4711.
22. Tsou HR, Overbeek-Klumpers EG, Hallett WA, et al. *J Med Chem*. 2005;48:1107–1131.
23. Wu CH, Coumar MS, Chu CY, et al. *J Med Chem*. 2010;53:7316–7326.
24. Zegzouti H, Zdanovskaia M, Hsiao K, Goueli SA. *Assay Drug Dev Technol*. 2009;7:560–572.
25. Nishii R, Volgin AY, Mawlawi O, et al. *Eur J Nucl Med Mol Imaging*. 2008;35:990–998.